

Conformational selection mechanism governs oxygen ligation to H-NOX proteins

Dóra K. Menyhárd

Institute of Chemistry, Eötvös Loránd University, Pázmány P. sétány 1/A, H-1117 Budapest, Hungary.

e-mail: dmenyhard@chem.elte.hu

ABSTRACT :

H-NOX proteins are at present the only structural models available for the study of the ligand binding affinity and selectivity of soluble guanylate cyclase, the physiological receptor of nitric oxide. The oxy complex and resting state structures of two bacterial H-NOX proteins of markedly different oxygen affinity, but of quite similar sequence, were studied by molecular dynamics simulations at 300K and 400K. Unexpectedly, the different O₂ affinity was found to be reflected in differences of the resting states structures. A conformation containing a pre-formed oxygen-binding cage is the most populated in the resting state equilibrium ensemble of the only successful O₂ binder, Tt H-NOX at 300K, suggesting that conformational selection governs the interaction.

Nitric oxide is a key signaling molecule of our physiology. By activating its receptor, soluble guanylate cyclase (sGC), it takes part in the regulation of various processes of the nervous, muscular, cardiovascular and immune systems [1, 2]. The two hundred fold amplification of sGC's synthesis of cGMP upon NO ligation to its heme iron is thus the launch of several vital reaction cascades [3] – the selectivity and specificity of its activation signal is therefore of crucial significance. sGC fulfills this requirement by possessing a high affinity for NO and at the same time not binding O₂ at all, a remarkable feat, considering the thousand fold excess of the latter and the similarity in both size and composition of the two. Furthermore, the heme and its coordination to the protein matrix in this enzyme are analogous to those of the globins, the main storage and transport proteins of oxygen. The molecular details of O₂ exclusion were thought to be clarified by predicting, based on the crystal structure of a bacterial homologue (H-NOX protein from *Thermoanaerobacter tengcongensis* (Tt H-NOX) [4-5]), the active site pocket of sGC to be completely apolar, thus unable to stabilize the dipole created when O₂ is bound to the heme iron, while being quite adequate for hosting the neutrally coordinated physiological ligand, NO [6]. Tt H-NOX, on the other hand, originates from an anaerobe species, unequipped for discrimination against O₂, accordingly, on air, it forms a stable oxy-complex [4, 5], while the resting state of sGC is a five coordinate ferrous deoxy-state [7]. The partial negative charge of the heme-bound O₂ in Tt H-NOX is stabilized by a Tyr residue of the distal pocket, which is present in all known anaerobe sGC homologues, while is absent in sGC and its facultative aerobic relations. At the same position in the sGC sequence an Ile can be found – the accepted model for selectivity thus focuses on the presence or absence of a proton donor within the active pocket which would or would not stabilize the heme bound oxygen.

This notion was supported by a mutational study, where it was shown that i.) mutating the Tyr residue of the Tt H-NOX active pocket to Leu considerably reduces its oxygen affinity, and also that ii.) the replacement of the implicated Ile by a Tyr residue in the heme-binding domain fragment of sGC resulted in the reverse, the introduction of O₂ binding ability [6]. However, in the reconstituted full enzyme this latter mutation did not facilitate oxygen binding [8]. It was also shown that Tt H-NOX loses its oxygen binding ability at higher temperatures, and forms a stable NO complex even in the presence of oxygen [4]. A further challenge was the finding that another H-NOX protein, that from *Clostridium botulinum* (Cb) sharing 39% sequence identity with Tt H-NOX, although it contains the implicated Tyr

residue, is an even more acute – femtomolar - NO sensor (thus O₂ excluder) than sGC [4]. This directly contradicts the original hypothesis which explains the selectivity of sGC by the absence of this specific Tyr. Thus, considerable ambiguity still persists as to whether the presence of Tyr, or any other H-bond donor in the distal heme pocket is, and is the only prerequisite of O₂ binding, and its absence the guarantee of selectivity. The results of present MD simulations allowed for the comparison of the resting and oxy-complex states of *Tt* H-NOX at two different temperatures as well as those of *Cb* H-NOX, and indicate that it is not the structure of the oxy complexes that differentiate the oxygen disclosing ability of these proteins but their resting state structures, especially the different extent of solvation of their respective active pockets, which creates a markedly different welcome for the arriving oxygen molecules from (basically) the same protein building blocks.

Since the crystal structure of sGC has not been determined yet, structural details of its activation mechanism can only be studied using the bacterial homologues of its heme-containing, NO binding domain. The crystal structure of the oxy complex of *Tt* H-NOX was determined at low temperature where it is an O₂ binder instead of an excluder [4, 5], and the structure of its ferric, water-ligated state was also established [5]. These, nearly identical structures were used for the calculations concerning *Tt* H-NOX and for building a homology model (using the Modeller program [9]) for the *Cb* H-NOX protein, for which a crystal structure is not available. 25 ns NVT MD simulations were carried out to model the resting state structure and oxy complex of *Tt* H-NOX at 300K and 400K and those of *Cb* H-NOX. The GROMACS program suite [10] and CHARMM27 force field [11, 12] was utilized. Parameterization and charge assignment of the heme and the oxygen ligand was carried out using the geometries available in crystal structures and by QM/MM calculations (using QSite [13] and ESP charges from B3LYP/LACVP*/OPLSAA wavefunctions). Systems were solvated by approx. 20000 TIP3P waters, protein overall charge was neutralized and physiological salt concentration set by Na⁺ and Cl⁻ ions. Average geometries and B-factors were calculated using the last 10 ns of the trajectories.

Tt H-NOX is a globular protein. It contains 7 α -helices (named A-F) and a 4-stranded anti-parallel β -sheet (with β -strands numbered 1-4). Naturally, the most mobile regions of the protein are the loops connecting the secondary elements, but the flexibility of two loops, that of α F β 1 (residues 105-115) and the facing α B α C loop (residues 24-42) might have catalytic significance too, since these loops have been indicated as gate-keepers of the ligand entrance region in *Tt* H-NOX [14, 15]. The B-factor distribution along the sequence was found to be essentially the same both in the different crystal structures and in previous [14, 16] and present MD studies. Figure 1 shows the backbone B-factors obtained in this study as compared with those of the crystal structures. The simulations also sufficiently reproduced the overall conformation seen in the crystal structures of *Tt* H-NOX and oxy-*Tt* H-NOX, with a backbone rms deviation of 1.7 Å and 2.4 Å, respectively (calculated using the average structure of the equilibrium trajectory), which is comparable to the rms deviation between structures from different crystal forms (for example, the rms of 2.0 Å between the PDB entries 1u55 [5] and 1xbn [4]).

All three models were forced into the oxy-complex state by covalently linking the oxygen molecule to the heme iron, thus the calculations pertaining to this form show not the oxygen affinity of the species but how the protein matrix would adapt to the presence of the oxygen molecule, if it was bound. As can be seen in Figure 2 and Table S1, although the overall conformation shows variances, especially in the loop regions, the active site and the mode of oxygen coordination is, in spite of their characteristically different oxygen affinities – unexpectedly - quite similar in oxy-*Tt* H-NOX (300K), oxy-*Tt* H-NOX (400K) and in the oxy-*Cb* H-NOX structure. In all three cases, as in the crystal structure of oxy-*Tt* (300K) too

[4, 5], the Tyr140 (numbering according to *Tt* H-NOX) residue of the distal active pocket forms an H-bond [17] with the heme bound O₂, in the 94.0%, 87.4% and 98.6% of the snapshots of the equilibrium trajectory, in oxy-*Tt* H-NOX (300K), oxy-*Tt* H-NOX (400K) and in the oxy-*Cb* H-NOX structures, respectively. Tyr140 is stabilized by favorable interactions with the nearby Asn74 and Trp9 residues.

In resting state, all three models incorporate a water molecule as the sixth, axial ligand of the heme iron after about 8 ns of simulation time (see Figure3 and Table S1) – resulting in an arrangement that is seen in the crystal structure of ferric *Tt* H-NOX (300K) too [5]. Waters succeeding to the heme iron enter via the proposed entrance gate and are permanently bound in case of *Tt* H-NOX (300K) and *Cb* H-NOX. In case of *Tt* H-NOX (400K), although the sixth, ligand binding position is always occupied (99.9% of snapshots), the water molecules exchange fast – rarely spend more than 1 ns at the iron. In *Tt* H-NOX (300K) the heme bound water molecule is H-bonded by Tyr140 in 78.5% of the snapshots. Tyr140 behaves as a proton donor in approx. 40% of the cases (these resemble the crystal structure more closely), while as a proton acceptor in the rest and subsequently donates its proton to Asn74 which reaches with its amide oxygen toward the Tyr hydroxyl in these structures (see Figure 3). These two conformers – State I and State II of *Tt* H-NOX (300K), respectively – share quite similar backbone structures (rms: 1.0 Å), and interchange into one-another along the trajectory.

In case of *Cb* H-NOX, 300 ps after the arrival of the first water (Wat1), a second one appears above pyrrole A of the heme (Wat2). In *Tt* H-NOX, this spot is not available for water binding, it is covered by an isoleucine, Ile5, which hovers above the heme plane and distracts waters, while in *Cb* H-NOX, a less bulky residue, a Val is found in this position, which leaves enough space for water coordination. It is interesting to note, that Ile5 of *Tt* H-NOX is the only residue of its active site pocket that takes up characteristically different conformations even within a crystal lattice (in chain A and B of both 1u55 and 1u56) and was also proposed to exert influence over heme distortion [5]. In *Cb* H-NOX Wat2 becomes the prime H-bond partner of Tyr140, in 98.0% of the snapshots Tyr donates its hydroxyl proton to form an H-bond with it. The Tyr – Wat1 H-bond is preserved in only 9.8% of the snapshots, while in the majority of cases (69.1%), Wat1 is stabilized above the heme iron by an H-bond toward the amide oxygen of Asn74. For this end, Asn74 is shifted and flipped; its amide oxygen intrudes into the ligand binding zone. The active site thus created is quite unfavorable for O₂ binding, since the negatively polarized oxygen of Asn74 is just as close to the ligand binding site as the potential H-bond donor Tyr140, which, in this arrangement is unavailable for proton donation.

In *Tt* H-NOX (400K) yet another situation is encountered. Here at least one further water molecule is inserted between the heme iron and the Tyr in most structures. Both the iron-close and the Tyr site is occupied in nearly all snapshots (99.9%, 90.5%, respectively), however, these two waters are only the same in 4% of the cases. Water molecules exchange rapidly at both sites, those solvent molecules that eventually reach the heme iron usually temporarily ligate to Tyr140 too, either when approaching or when leaving the iron-site. Thus in this case, Tyr is pushed out of the H-bond reach of the heme-bound ligand, and is again unavailable for proton donation.

Based on the calculated structures and the experimental evidence regarding their O₂ affinity, it can be concluded that the only successful O₂ binder, *Tt* H-NOX (300K), is the one where the water ligand of the resting state is stabilized by the protein matrix the same way as the oxygen molecule of its oxy-complex. Therefore, the availability of an H-bond donor in the ligand binding pocket of H-NOX proteins seems a necessary but not sufficient condition of O₂ binding; instead, the requirement would be the presence of a well positioned proton donor in an equilibrium ensemble that samples dominantly the conformation corresponding to

a pre-formed O₂ capturing cage. The significance of the resting state conformation was thus far overlooked, since the crystal structure of the water-bound ferric form of *Tt* H-NOX and its ferrous oxy complex are virtually identical (backbone rms of 0.43 Å), suggesting that all similar matrices would behave the same. Very subtle changes lead to the alteration of the average resting state structures in the present results, an Ile/Val change in case of *Tt* vs. *Cb* H-NOXs, or the elevation of temperature (*Tt* H-NOX (300K) vs. *Tt* H-NOX (400K)) which indicates that the pre-formed oxygen-binding conformation is easily disrupted. Something similar might happen in case of sGC too, where contradictory evidence was generated using just the oxidative, heme containing domain and the full-length enzyme regarding the significance of the Ile/Tyr mutation on oxygen affinity [6, 8]. Heterodimerization can easily result in a shift in the population of resting state conformers reducing the representation of the conformer favoring O₂ binding, thus creating a different affinity in the full-length enzyme. This finding can be supported by recent experimental results. Although a Tyr residue incorporated in itself into the sequence could not turn the full-length enzyme into an oxygen binder, a stable oxy complex was recently obtained by a double mutation; Ile145 was mutated to a Tyr (in place of the Tyr140 of *Tt* H-NOX), and its through-space neighbor, Ile149 was mutated to Gln [18]. The corresponding residue of this latter in *Tt* H-NOX is Leu144, which reaches above heme pyrrole C, thus the presumed hydrogen bonding interaction between the Tyr and the Gln of the double mutant would restrict the Tyr to a heme-iron-close position. The fact that only this variant is capable of O₂ binding suggests that fixing the Tyr in a correct O₂ ligating position is a vital prerequisite of oxy-complex formation, as was indicated by the present results also.

In summary – present simulation results indicate that oxygen will not induce its fit within the H-NOX active pocket, instead a conformational selection scenario governs the association. In case of *Cb* H-NOX and *Tt* H-NOX (400K), the “oxy-complex-like” conformation (H-bond between iron-bound water and the Tyr and a sufficiently removed amide oxygen of Asn) is scarcely represented in the resting state (1.7% in *Cb* H-NOX, 4.0% in *Tt* H-NOX (400K)), thus the binding event does not take place. In case of *Tt* H-NOX, the conformation containing a pre-formed oxygen-binding cage is the most populated of the resting state equilibrium (78.5%) and this is what leads to complexation. Results also show that finding a Tyr residue in the distal heme pocket of highly selective *Cb* H-NOX, does not contradict the widely accepted hypothesis which points to the absence of a proton donor in the active pocket as the cause of its NO/O₂ selectivity, and indicate that oxygen exclusion from the active site can be possible even in its presence. Thus, the results reinforce the applicability of the currently used structural model for the description of sGC’s selectivity which was extenuated by being unable to explain the temperature dependence of the oxygen affinity of *Tt* H-NOX and O₂ exclusion from *Cb* H-NOX.

ACKNOWLEDGMENT Author thanks Veronika Harmat for helpful discussions. Financial support of OTKA grant numbers NI68466, and NK67800 as well as of ICGEB CRP/HUN09-03 is gratefully acknowledged.

Supporting Information Available: Table S1. Characteristic inter-atomic distances of the average structures of the trajectories. Heme parametrization.

REFERENCES

1. Moncada, S.; Palmer, R. M.; Higgs E. A. *Pharmacol. Rev.* 1991, 43, 109.

2. a. Nathan, C. *FASEB J.* 1992, 6, 3051., b. Berdeaux, A. *Fund. Clin. Pharmacol.* 1993, 7, 401.
3. Koesling, D.; Russwurm, M.; Mergia, E.; Mullershausen F.; Friebe, A. *Neurochem. Int.* 2004, 45, 813.
4. Nioche, P.; Berka, V.; Vipond, J.; Minton, N.; Tsai, A-L.; Raman, C. S. *Science* 2004, 306, 1550.
5. Pellicena, P.; Karow, D. S.; Boon, E. M.; Marletta, M. A.; Kuriyan, J. *Proc. Natl. Acad. Sci USA* 2004, 101, 12854.
6. Boon, E. M.; Huang S. H.; Marletta, M. A. *Nature Chem. Biol.* 2005, 1, 53.
7. Stone, J. R.; Marletta M. A., *Biochemistry* 1994, 33, 5636.
8. Martin, E.; Berka, V.; Bogatenkova, E.; Murad F.; Tsai, A-L. *J. Biol. Chem.* 2006, 281 27836.
9. Eswar, N.; Marti-Renom, M. A.; Webb, B.; Madhusudan, M. S.; Eramian, D.; Shen, M.; Pieper U.; Sali A. *Current Protocols in Bioinformatics*; John Wiley & Sons, Inc., 2006, Supplement 15, 5.6.1-5.6.30.
10. van der Spoel, D.; Lindahl, E.; Hess, B.; Groenhof, G.; Mark, A. E.; Berendsen, H. J. C. *J. Comp. Chem.* 2005, 26, 1701.
11. MacKerell Jr., A. D.; Feig, M.; Brooks, C. L. *J. Comput. Chem.* 2004, 25, 1400.
12. Bjelkmar, P.; Larsson, P.; Cuendet, M. A.; Hess B.; Lindahl, E. *J. Chem. Theory Comput.* 2010, 6, 459.
13. Murphy, R. B.; Philipp, D.M.; Friesner, R. A. *J. Comp. Chem.* 2000, 21, 1442.
14. Zheng, Y.; Lu, M.; Chen, Y.; Li, Z. *J. Mol. Graph. Mod.* 2010, 28, 814.
15. Olea Jr., C.; Herzi, Jr., M. A.; Kuriyan J.; Marletta, M. A. *Protein Sci.* 2010, 19, 881.
16. Capece, L.; Estrin, D. A.; Marti, M. A. *Biochemistry* 2008, 47, 9416.
17. The criteria used for determining the presence of an H-bond: donor-acceptor heteroatom distance less than 3.2Å, and hydrogen – acceptor distance less than 2.2 Å
18. Derbyshire, E. R.; Deng, S.; Marletta, M. A. *Biochemistry* 2010, 285, 17471.

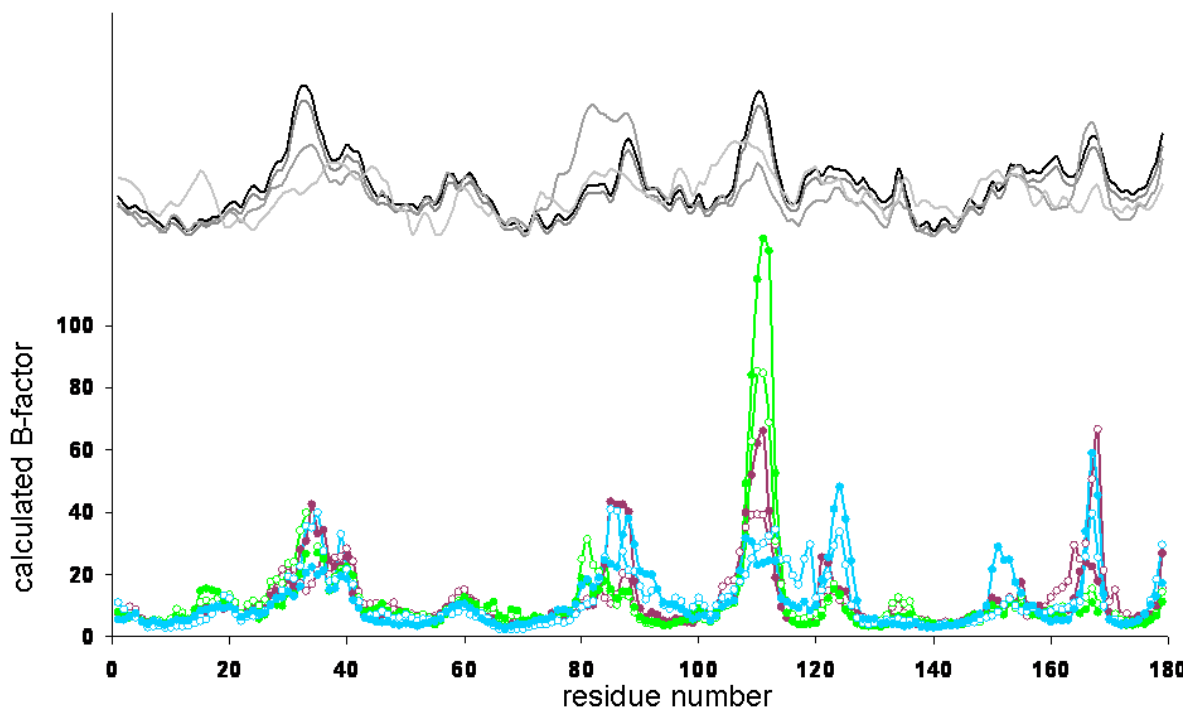


Figure 1. Crystallographic and calculated B-factors. Crystallographic B-factors were shifted up for clarity, and are colored from black to lighter grey, for those of PDB code 1u56, 1u55, 1u4h, 1xbn, respectively. B-factors of *Tt* H-NOX (300K) are in purple, *Tt* H-NOX (400K) in cyan and *Cb* H-NOX in green. Oxy-complexes are shown in full circles, resting state results by empty circles.

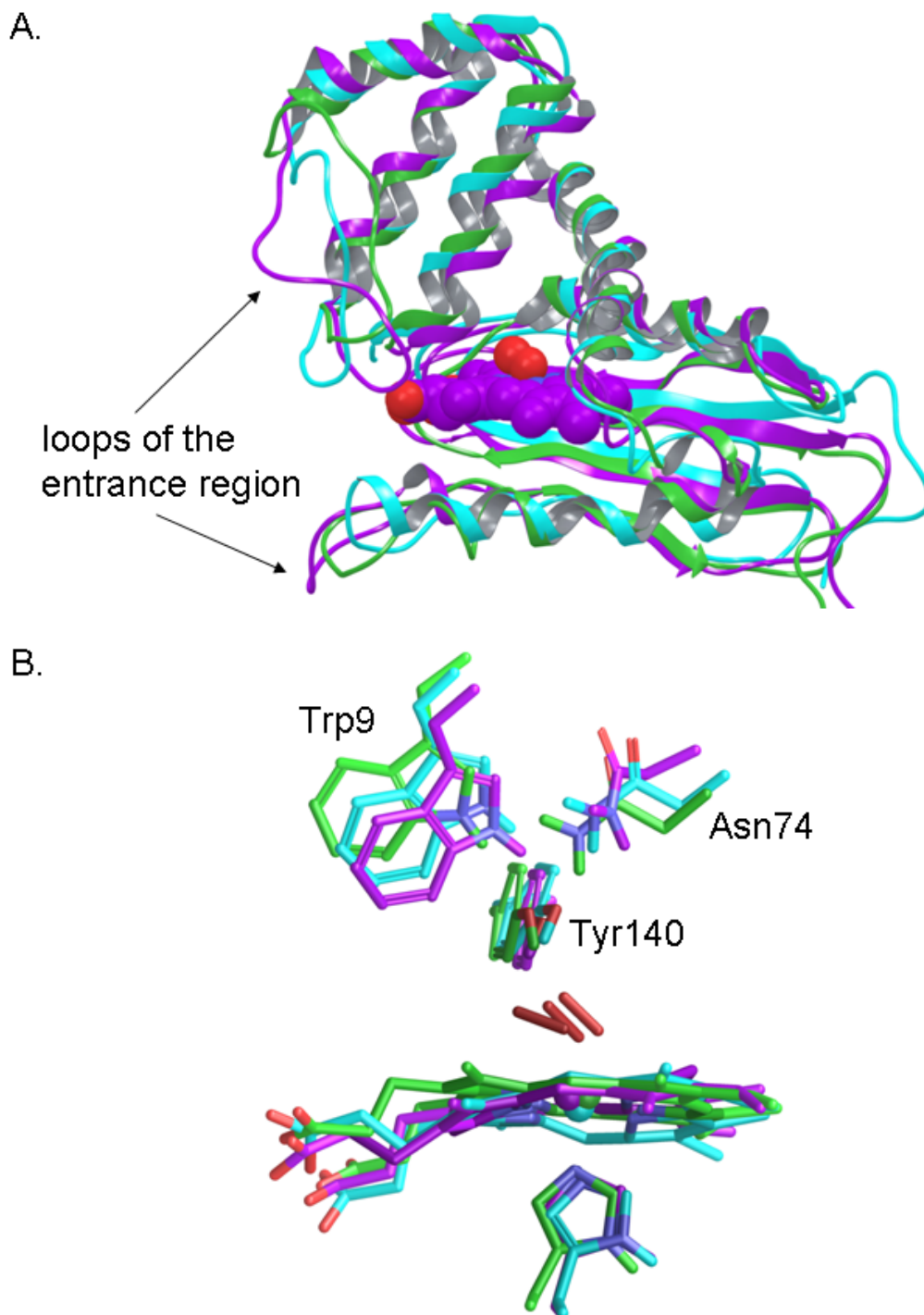


Figure 2. Calculated structures of the oxy complexes. *Tt* H-NOX (300K) atoms and backbone trace is shown in purple, *Tt* H-NOX (400K) in cyan and *Cb* H-NOX in green (following the color scheme of Figure 1). A. Average structure of the trajectories (only *Tt* H-NOX (300K) heme shown explicitly, for clarity). B. Close-up of the heme site (in a snapshot most resembling the average structure).

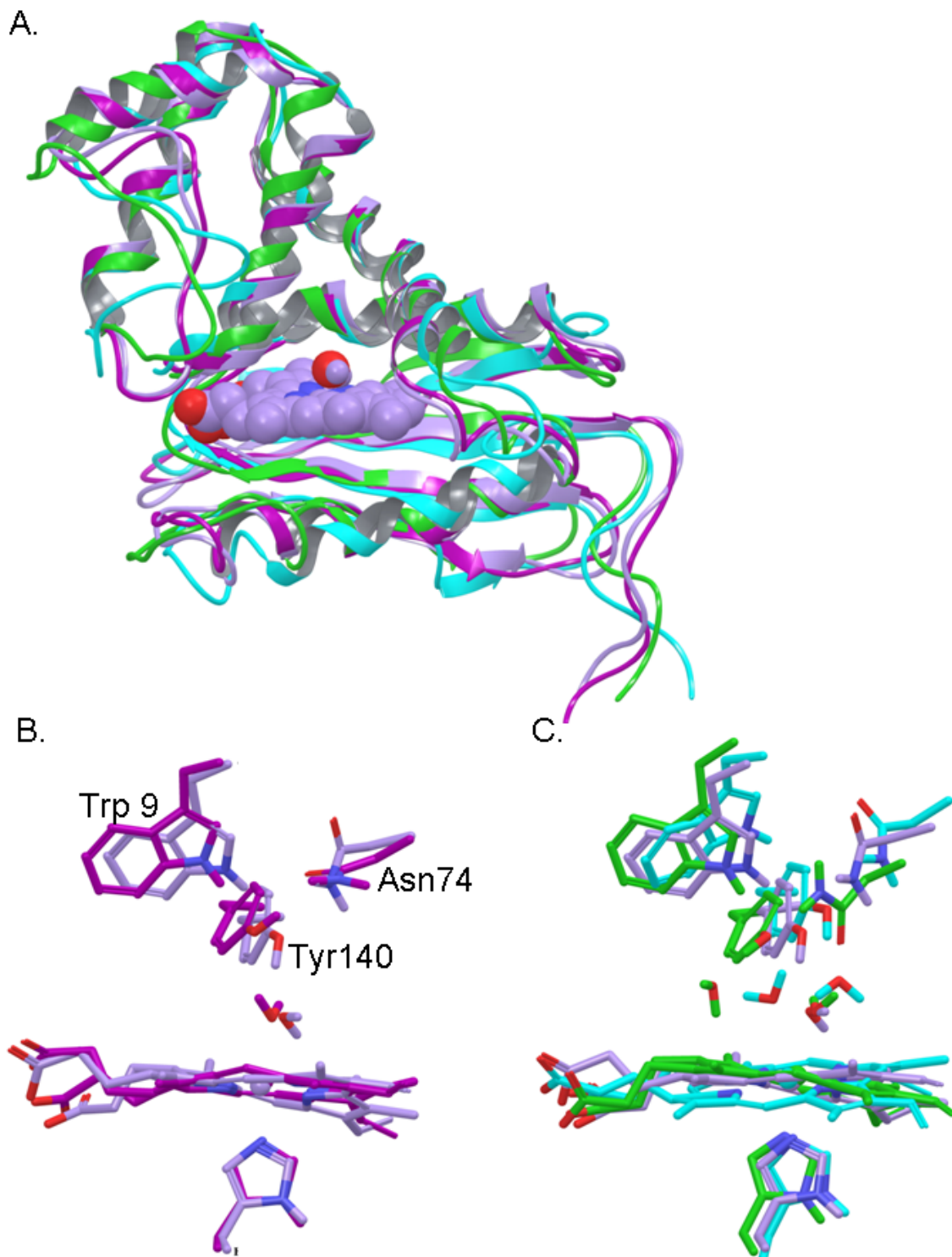


Figure 3. Calculated structures of the resting state complexes. *Tt* H-NOX (300K) atoms and backbone trace is shown in two shades of purple, State I in lighter, State II in darker, *Tt* H-NOX (400K) in cyan and *Cb* H-NOX in green (following the color scheme of Figure 1). A. Average structure of the trajectories (only *Tt* H-NOX (300K) State I heme shown explicitly, for clarity). B. Close-up of the heme site, comparing State I and II of *Tt* H-NOX (300K). C.

Comparison of the heme sites of *Tt* H-NOX (300K) State I, *Tt* H-NOX (400K) and *Tt* H-NOX (in a snapshot most resembling the average structure).